Korean J. Chem. Eng., 32(9), 1749-1758 (2015)
DOI: 10.1007/s11814-015-0003-4

pISSN: 0256-1115
eISSN: 1975-7220

Instantaneous NO release from ellipsoidal particles during char combustion in a hot gas with fluctuating temperature

Jie Li† and Jian Zhang

Department of Engineering Mechanics, Tsinghua University, Beijing 100084, China
(*Received 4 November 2014 • accepted 31 December 2014*)

Abstract−We have established the instantaneous governing equations for NO release during char combustion of non-spherical particles theoretically. The instantaneous released NO mass variations, the instantaneous char oxidation reaction rates, and the instantaneous NO reduction reaction rates of char particles were computed numerically under different fluctuation amplitudes of gas temperature, kinetic parameters of char oxidation reaction and NO reduction reaction, and particle aspect ratios. The gas temperature fluctuation results in a faster NO release rate, a faster char oxidation reaction rate, and a faster NO reduction reaction rate during the whole char combustion processes. The activation energy of char oxidation reaction has obvious influence on the NO release and char combustion processes. The kinetic parameters of NO reduction reaction have no contribution to the conversion time. Under the same particle surface area, the conversion rate of char nitrogen to NO increases with the increase in the particle aspect ratio.

Keywords: Gas Temperature Fluctuation, Ellipsoidal Particle, Aspect Ratio, NO Release, Char Combustion

INTRODUCTION

The combustion of solid fuel in a furnace will accompany pollutant emissions [1,2]. As one of the primary industrial gaseous wastes, nitrogen oxides (NO_x) with high concentration usually lead to photochemical smog, acid rain, ozone depletion, and diseases of respiratory system [3]. A number of control techniques, such as catalytic reduction, staged combustion, reburn combustion, and co-firing with renewable fuels, have been proposed to reduce gaseous emissions [4]. The operating costs and maintenance costs of some control methods are relatively high, and therefore development of new combustion technologies is driven continuously. A better understanding of the pollution behaviors will be helpful in the development of combustion technology with low pollutant emission.

The majority of NO_x originates from the fuel nitrogen, which includes the volatile nitrogen and the char nitrogen. The heterogeneous reaction rates of the char nitrogen relate directly to the instantaneous particle temperature, and that is influenced by the gas temperature, which exhibits turbulent fluctuations in the flow field [5]. Zhang et al. explored the effects of gas temperature fluctuation on the instantaneous NO release from pulverized coal particles during the char combustion [6]. The instantaneous NO release mass variations were numerically computed. The results showed that the gas temperature fluctuation led to a faster NO release rate and a shorter char burning time Similarly, the influences of fluctuating temperature on the instantaneous char reaction of pulverized coal particles, the instantaneous devolatilization of pulverized coal particles, and the instantaneous pyrolysis of biomass particles have been studied [7-9]. It was found that the particle diameter, the time-averaged gas temperature, and the particle Reynolds number have obvious influences on the instantaneous combustion processes [6-9]. Note that the kinetic parameters (activation energy and pre-exponential factor) of char oxidation reaction and NO reduction reaction vary over a wide range, depending on the fuel type and the measurement precision. Thus it is necessary to further explore the effects of kinetic parameters on the NO release.

Most previous studies treated the fuel particles as spherical particles in the theoretical models [10-13]. However, the studies of microstructure of the solid fuel observed by the scanning electron microscope showed that the particles generally are irregular-shaped [14,15]. Pulverized coal particles tend to be near-spherical or prolate spheroidal particles with sphericity around 0.6-0.9, while straw and switchgrass particles are approximately described as cylinder particles [16,17]. The various particle shapes make it unreasonable to directly borrow the previous theoretical knowledge for non-spherical particles.

We used the ellipsoidal coordinate system to establish theoretically the energy equations for NO release during char combustion of prolate spheroidal particles. To further explore the transient responses of the fluctuation amplitude of the gas temperature and the kinetic parameters to the NO release during the char oxidation processes of ellipsoidal particles, the instantaneous released NO mass variations, the instantaneous char oxidation reaction rates, and the instantaneous NO reduction reaction rates were numerically computed. The gas flow was assumed to have a uniform but fluctuating temperature.

INSTANTANEOUS ENERGY EQUATIONS

The char oxidation reaction, the char nitrogen oxidation reaction, and the NO_x reduction reaction are considered during the char combustion processes. It is assumed that the primary NO_x on the particle surface is NO. The following global surface reactions were adopted:

†To whom correspondence should be addressed.
E-mail: leejay1986@163.com

$$C(s)+1/2O_2(g)\rightarrow CO(g) \quad (1a)$$

$$N(s)+1/2O_2(g)\rightarrow NO(g) \quad (1b)$$

$$C(s)+NO(g)\rightarrow CO(g)+1/2N_2(g) \quad (1c)$$

The instantaneous energy equation for a single char particle can be expressed as [10]

$$m_k\frac{dh_k}{dt}=O_{ck}+Q_{rk}+Q_{CO} \quad (2)$$

where Q_{ck}, Q_{rk}, Q_{CO} denote the convective heat transfer between the char particle and gas, the radiative heat transfer between the char particle and the combustor wall, and the heat generation due to the heterogeneous char oxidation reaction, respectively. h_k is the particle enthalpy. The heat of char nitrogen oxidation reaction and the heat of NO reduction reaction were not considered, as the char oxidation reaction rate is far greater than both the oxidation reaction rate of char nitrogen and the NO reduction reaction rate. In addition, the heat release of the heterogeneous oxidation reaction of char nitrogen has the same order of magnitude as the heat absorption of the NO reduction reaction.

Considering the geometry of the ellipsoidal particle, the above four terms are further expressed as

$$m_k\frac{dh_k}{dt}=\frac{4}{3}\pi ab^2\rho_{pk}C_{pk}\frac{dT_k}{dt} \quad (3a)$$

$$Q_{ck}=\pi d_k\frac{B_k}{\exp(B_k)-1}Nu_k\lambda(T-T_k) \quad (3b)$$

$$Q_{rk}=\pi d_k^2\varepsilon_k\sigma_b(T_w^4-T_k^4) \quad (3c)$$

$$Q_{CO}=G_{CO}q_{CO} \quad (3d)$$

where a and b are the semi-axes of ellipsoidal particle (a>b=c), B_k is the nondimensional variation rate of particle mass given by $B_k=-G/(\pi d_k Nu_k\lambda/C_p)$, q_{CO} represents the heat of char oxidation reaction, ε_k denotes the particle emissivity, and T_w represents the combustor wall temperature. G_{CO} and G are the char oxidation reaction rate and the total mass flow rate on the particle surface, respectively. d_k is the diameter of a spherical particle having the same external surface area, which is written as

$$d_k=\left(2b^2+\frac{2a^2b}{\sqrt{a^2-b^2}}\arcsin\frac{\sqrt{a^2-b^2}}{a}\right)^{1/2} \quad (4)$$

Nu_k denotes the particle Nusselt number [18]:

$$Nu_k=2^{3/2}\sqrt{M^2-1}\left(ar\coth\sqrt{\frac{M^2}{M^2-1}}\right)^{-1}\left(1+\frac{2a^2bM^2}{\sqrt{M^2-1}}\arcsin\frac{\sqrt{M^2-1}}{M}\right)^{-1/2} \quad (5)$$

where M=a/b is the aspect ratio of the ellipsoidal particle.

INSTANTANEOUS REACTION RATES

1. Char Oxidation Reaction Rate

The instantaneous char oxidation reaction rate is governed by the diffusion-kinetic controlled regime. The heterogeneous chemical kinetics gives [19]

$$G_{CO}=-\frac{1}{\beta_{CO}}\pi d_k^2p_s\frac{M_s}{M_{OX}}Y_{OX,s}B_{CO}\exp\left(-\frac{E_{CO}}{RT_k}\right) \quad (6)$$

where β_{CO} is the stoichiometric ratio for reaction (1a). p_s, M_s, M_{OX}, $Y_{OX,s}$ are the gas pressure, the mixed gas molecular weight, the oxygen molecular weight, and the oxygen mass fraction on the particle surface, respectively. B_{CO}, E_{CO}, R are the pre-exponential factor, the activation energy of char oxidation reaction, and the universal gas constant, respectively.

The ellipsoidal coordinate system is introduced to derive the oxygen mass fraction on the particle surface. The surface of an ellipsoid is a quadric surface which satisfies the equation $x^2/a^2+y^2/b^2+z^2/c^2=1$. The ellipsoidal coordinates (ξ, η, ζ) are defined as the solutions of the equation $x^2/(a^2+s)+y^2/(b^2+s)+z^2/(c^2+s)=1$. Appendix A describes the ellipsoidal coordinate system in detail. The oxygen mass conservation in steady flow in terms of ellipsoidal coordinates can be expressed as (see Appendix A)

$$\frac{\partial}{\partial\xi}(gY_{OX}R_\xi H_\eta)=\rho D\frac{\partial}{\partial\xi}\left(R_\xi\frac{\partial Y_{OX}}{\partial\xi}\right) \quad (7)$$

where g denotes the mass flux on the ellipsoid surface. R_ξ and H_ξ are scale factors defined in the ellipsoidal coordinate system. ρ and D are the gas density and the diffusion coefficient. The boundary conditions for Eq. (7) are $Y_{OX}(\xi=0)=Y_{OX,s}$ and $\partial Y_{OX}/\partial\xi(\xi=0)=(\partial Y_{OX}/\partial\xi)_s$. Using this knowledge, Eq. (7) is integrated to yield:

$$g(Y_{OX}R_\xi-Y_{OX,s}R_{\xi=0})=\rho DR_\xi H_\xi^{-1}\partial Y_{OX}/\partial\xi-\rho DR_{\xi=0}(H_\xi^{-1}\partial Y_{OX}/\partial\xi)_s \quad (8)$$

The theory of Stefan flow is associated with Fick's law of diffusion and the mass flux [19], which yields:

$$g_{OX}=gY_{OX,s}-\rho D(\partial Y_{OX}/\partial n)_s \quad (9)$$

where g_{OX} denotes the oxygen mass flux on the ellipsoid surface, and n is the unit vector outward normal to the ellipsoid surface. The relationship between $\partial Y_{OX}/\partial n$ and $\partial Y_{OX}/\partial\xi$ is proposed by Grow [20]:

$$\partial Y_{OX}/\partial n=H_\xi^{-1}\partial Y_{OX}/\partial\xi \quad (10)$$

Substituting Eqs. (9) (10) into Eq. (8) and rearranging yields:

$$abcg_{OX}=Y_{OX}R_\xi g-\rho DR_\xi H_\xi^{-1}\partial Y_{OX}/\partial\xi \quad (11)$$

The above equation is integrated over the ellipsoid surface:

$$\iint_{\Pi}abcg_{OX}ds=abcG_{OX} \quad (12a)$$

$$\iint_{\Pi}Y_{OX}R_\xi gds=abcY_{OX}\iint_{\Pi}gds=abcY_{OX}G \quad (12b)$$

$$\iint_{\Pi}\rho DR_\xi H_\xi^{-1}\partial Y_{OX}/\partial\xi ds=8abc(a^2+\xi)^{1/2}(b^2+\xi)^{1/2}(c^2+\xi)^{1/2}\pi\rho D\partial Y_{OX}/\partial\xi \quad (12c)$$

where Π denotes the surface of the concentric ellipsoidal particle, and G_{OX} is the oxygen mass flow rate on the particle surface. Substituting Eq. (12) into Eq. (11) yields:

$$G_{OX}=Y_{OX}G-8(a^2+\xi)^{1/2}(b^2+\xi)^{1/2}(c^2+\xi)^{1/2}\pi\rho D\partial Y_{OX}/\partial\xi \quad (13)$$

The boundary conditions for oxygen mass fraction are $Y_{OX}(\xi=0)=Y_{OX,s}$ and $Y_{OX}(\xi\rightarrow\infty)=Y_{OX,\infty}$. $Y_{OX,\infty}$ is the oxygen mass fraction in the surrounding environment. Then Eq. (13) is solved for the prolate spheroidal particle (a>b=c) as

$$G=4\pi\rho D\sqrt{a^2-b^2}\left(\text{ar coth}\sqrt{\frac{a^2}{a^2-b^2}}\right)^{-1}\ln\frac{Y_{OX,\infty}-G_{OX}/G}{Y_{OX,s}-G_{OX}/G} \quad (14)$$

The oxygen mass fraction on the particle surface can be further obtained as

$$Y_{OX,s}=G_{OX}/G+(Y_{OX,\infty}-G_{OX}/G)\left\{\exp\left[(4\pi\rho D\sqrt{a^2-b^2})^{-1}ar\coth\sqrt{\frac{a^2}{a^2-b^2}}G\right]\right\}^{-1} \quad (15)$$

The model verification on the char oxidation reaction rate of ellipsoidal particles is difficult to do, because there is no relevant experimental study on the char combustion characteristics of rigid ellipsoidal particles and few investigations provided particle shape information (like aspect ratio or particle sphericity). The experimental results on the burning of a single wooden particle are used in this paper as a reference [21,22]. The time for char burning was estimated using a charge-coupled device (CCD) camera. The particle size in the experiment was a=3.3 mm and b=0.825 mm. Fig. 1 compares the measured char burning time and the computed char burning time in the regime of controlled diffusion-limited combustion due to the lack of measured particle temperature. It shows that the model predictions are in better agreement with the measurements as the temperature of the ambient gas stream is 1,873 K. The char combustion rate in the regime of controlled diffusion-limited combustion leads to different prediction effects. The ratio of the diffusional mass transfer resistance and the kinetical mass transfer resistance was calculated. It was shown that the kinetical mass transfer resistance can be neglected as the temperature was 1,873 K [21]. Thus the absence of the kinetical mass transfer resistance resulted in a higher char combustion rate and a shorter char burning time. Besides the inevitable experimental errors, the primary cause that affects the prediction precision is the different particle shapes. The biomass fuels used in the experiment were cylindrical particles while the burning particles are considered as rigid ellipsoids in the computations.

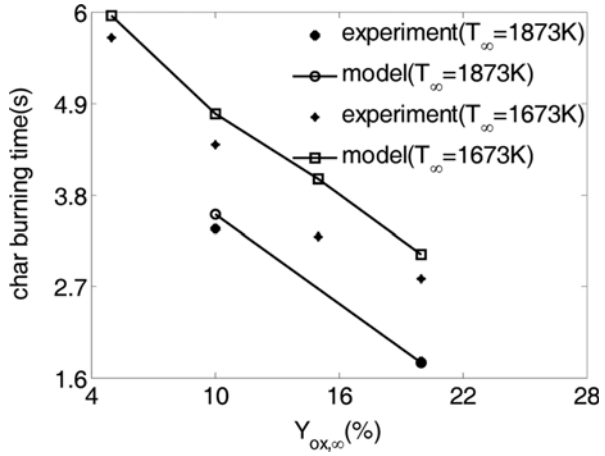

Fig. 1. Comparison of computed char burning times with experimental data.

2. Oxygen and Total Mass Flow Rates

As can be seen from Eq. (15), the oxygen mass fraction on the particle surface is associated with the oxygen and total mass flow rates on the particle surface. The mass flow rates relate to the rates of the heterogeneous reactions (1b) and (1c).

Similarly, the instantaneous NO reduction reaction rate is governed by the controlled diffusion-kinetic regime. The rate of NO reduction reaction (1c) is determined by [23]

$$G_{NO,2}=-\pi d_k^2 p_s M_s Y_{NO,s} B_{NO,2}\exp\left(-\frac{E_{NO,2}}{RT_k}\right) \quad (16)$$

where $B_{NO,2}$ and $E_{NO,2}$ are the pre-exponential factor and the activation energy of NO reduction reaction, respectively. $Y_{NO,s}$ is the nitric oxide mass fraction on the particle surface, which can be expressed as

$$Y_{NO,s}=G_{NO}/G+(Y_{NO,\infty}-G_{NO}/G)\left\{\exp\left[(4\pi\rho D\sqrt{a^2-b^2})^{-1}ar\coth\sqrt{\frac{a^2}{a^2-b^2}}G\right]\right\}^{-1} \quad (17)$$

where G_{NO} is the nitric oxide mass flow rate, and $Y_{NO,\infty}$ is the nitric oxide mass fraction in the surrounding environment.

The instantaneous char nitrogen oxidation reaction rate is assumed to be proportional to the instantaneous char oxidation reaction rate. The rate of heterogeneous reaction (1b) can be written as [24]

$$G_{NO,1}=-(1+\beta_{NO,1})\frac{Y_N}{Y_C}G_{CO} \quad (18)$$

where Y_N and Y_C are the nitrogen mass fraction and the carbon mass fraction in the fixed char, respectively. $\beta_{NO,1}$ is the stoichiometric ratio for reaction (1b).

The mass flows of oxygen and nitric oxide on the particle surface can be obtained as

$$G_{OX}=G_{OX,1}+G_{OX,2}=\beta_{CO}G_{CO}+\beta_{NO,2}\frac{Y_N}{Y_C}G_{CO} \quad (19a)$$

$$G_{NO}=G_{NO,1}+G_{NO,2} \quad (19b)$$

The total mass flow rate on the particle surface is then

$$G=\frac{1}{Y_C}G_{CO}+\frac{1}{\beta_{NO,2}}G_{NO,2} \quad (20)$$

where β_{NO2} is the stoichiometric ratio for reaction (1c).

CALCULATION CONDITIONS

The effect of gas temperature fluctuation on the instantaneous particle temperature is mainly reflected in the convective heat transfer term. The instantaneous gas temperature with a uniform spatial distribution is assumed in order to investigate the influence of gas temperature fluctuation on the NO release during the char com-

bustion. The instantaneous gas temperature is given by the following sine function as

$$T=T_{av}[1+A_t \sin(2\pi ft) \quad (21)$$

where T_{av}, A_t, f represent the time-averaged gas temperature, the fluctuation amplitude of the gas temperature, and the fluctuation frequency, respectively.

We numerically solved the instantaneous energy equations for the char combustion by the finite difference method. The first-order explicit scheme is used for the discretization of the instantaneous energy equation. The oxygen mass fraction and the nitric oxide mass fraction on the particle surface are calculated in an iterative way by utilizing Eqs. (14)-(20). The underrelaxation method is utilized in the computations of the oxygen mass fraction and the nitric oxide mass fraction on the particle surface.

A pulverized bituminous coal is chosen for the calculations. The char combustion is assumed to take place after the moisture and the volatile matter have evolved completely. Considering the solid fuel as a gray body, the radiation emission coefficient is taken as ε_k=0.8. The specific heat and the initial material density are taken as C_{pk}=1090 J/(kg·K) and ρ_{pk}=828 kg/m^3. The proximate analysis of the air dry basis is: moisture 1.4%, volatiles 31.08%, fixed char 56.22%, and ash 11.3%. The carbon and the nitrogen content in the fixed char are 80% and 0.4%, respectively. The char particles are considered to have an initial equivalent diameter of 50 μm. The initial aspect ratios are set to be 1, 3.25, and 4.6, respectively. We assumed the kinetic parameters of char oxidation reaction and NO reduction reaction are constants during the char combustion processes. The reference values of the kinetic parameters are given in the literature [23,25,26]. The gas thermal conductivity and the gas specific heat are calculated from the empirical correlations [19]. The oxygen and the nitric oxide mass fractions in the surrounding environment are set to be 0.1 and 1.058×10^{-3} (1,000 ppm), respectively. The particle initial temperature and the combustor wall temperature are set at 300 K. The time-averaged gas temperature is set to be 1,200 K. The typical value of the fluctuation frequency of the gas temperature is 100 Hz. The fluctuation amplitude of the gas temperature has typical values of approximately 0.1-0.2 in a combustion chamber [5]. The fluctuation amplitude of the gas temperature was chosen as 0, 0.1, and 0.2 in this study. The time step in all the computations is taken as 10^{-6} s.

RESULTS AND DISCUSSION

Figs. 2-7 present the effects of gas temperature fluctuation and kinetic parameters on the NO release during the char combustion processes. The aspect ratio is taken as M=1 in the computations. Fig. 2 shows the instantaneous released NO mass variations under the activation energy of char oxidation reaction of 77 kJ/mol, 80 kJ/mol, and 84 kJ/mol, respectively. The other kinetic parameters are given as B_{CO}=600 kg/(m^2·s·atm), $B_{NO,2}$=40 kmol/(m^2·s·atm), and $E_{NO,2}$=140 kJ/mol. For each calculation condition, the instantaneous released NO mass increases with time during the char combustion processes. The gas temperature fluctuation has evident influences on the instantaneous released NO mass variations. Compared with the results without the gas temperature fluctuation, the instantaneous released NO mass displays fluctuating variations with time. The gas temperature fluctuation leads to a faster increase in the released NO mass and a shorter char burning time. The increase in the fluctuation amplitude of the gas temperature from 0.1 to 0.2 further enhances the NO release rate and shortens the char burning time. The activation energy of char oxidation reaction has distinct effects on the instantaneous released NO mass variations. The NO release rate increases as the activation energy of char oxidation reaction decreases. With the increasing activation energy of char oxidation reaction, the conversion time varies from 0.253 s

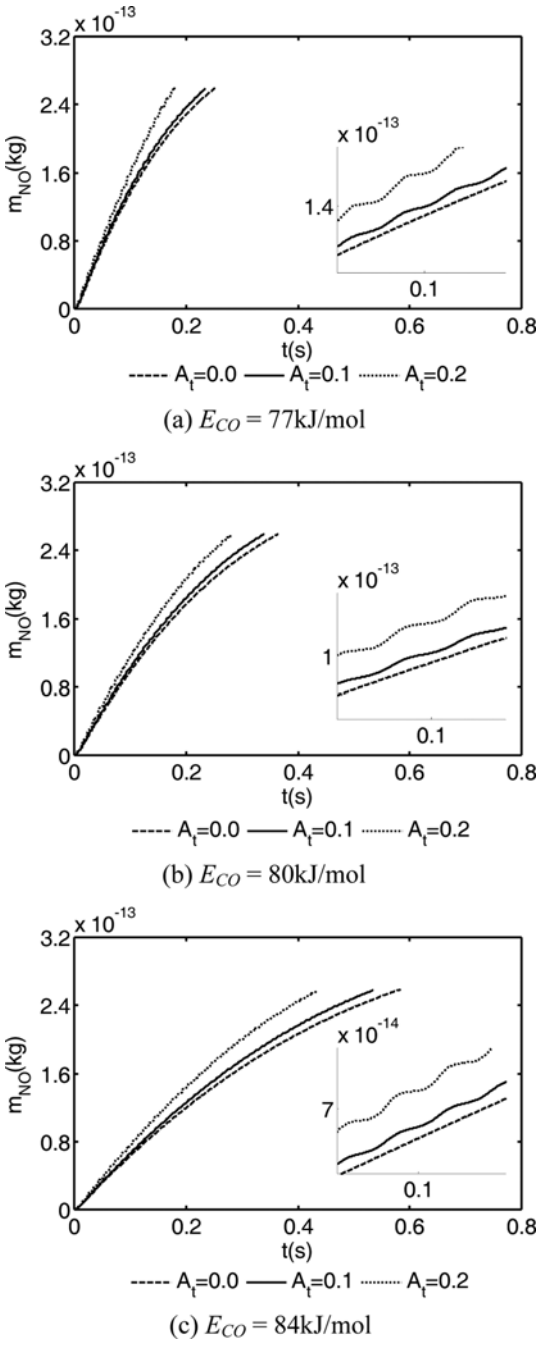

Fig. 2. Instantaneous released NO mass variations under different activation energies of char oxidation reaction.

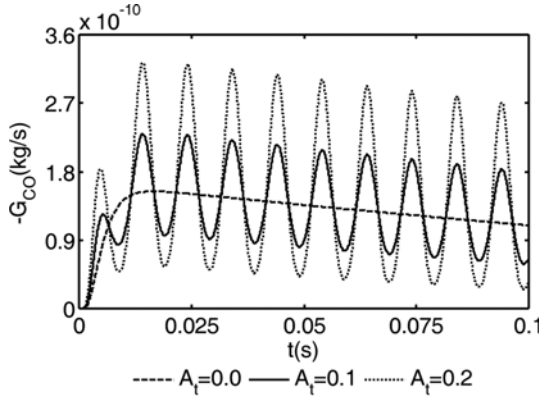

(a) E_{CO} = 77kJ/mol

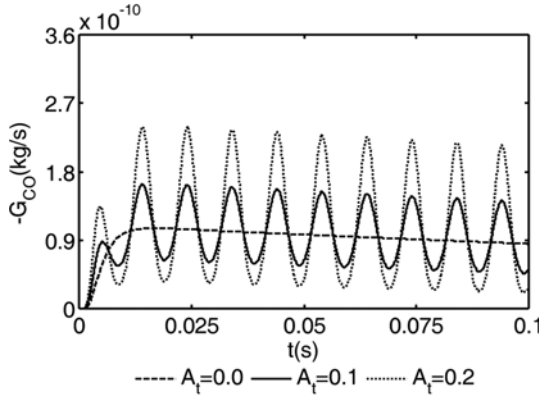

(b) E_{CO} = 80kJ/mol

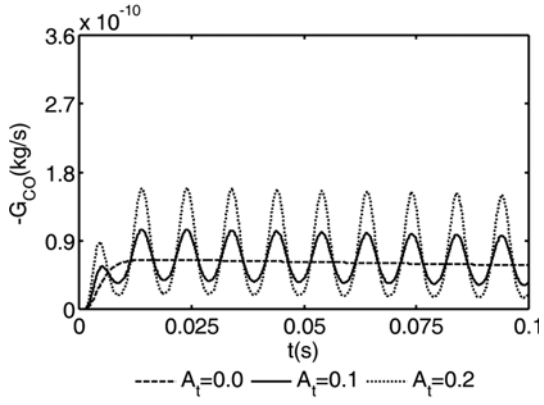

(c) E_{CO} = 84kJ/mol

Fig. 3. Instantaneous char oxidation reaction rate under different activation energies of char oxidation reaction.

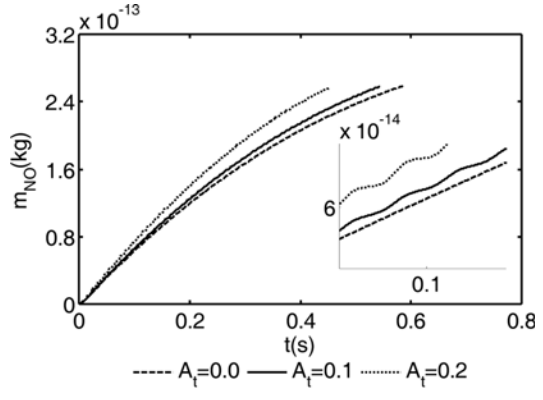

(a) B_{CO} = 400kg/(m^2·s·atm)

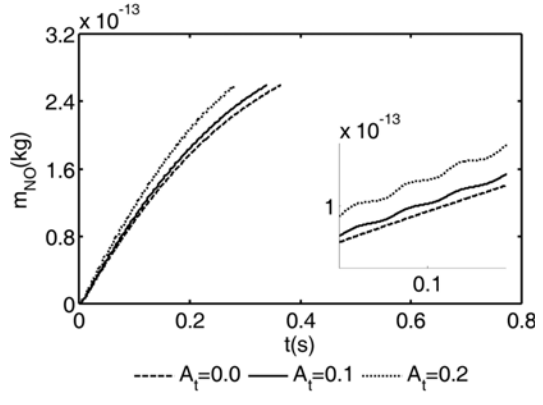

(b) B_{CO} = 600kg/(m^2·s·atm)

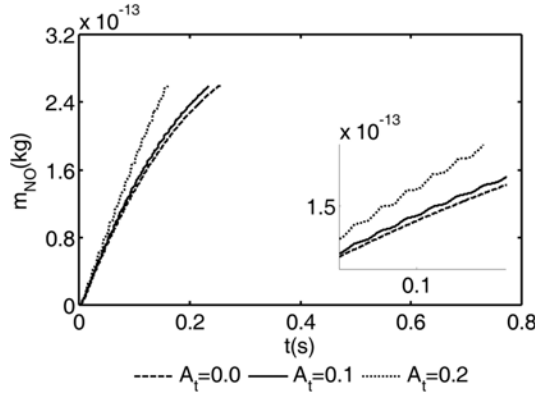

(c) B_{CO} = 800kg/(m^2·s·atm)

Fig. 4. Instantaneous released NO mass under different pre-exponential factors of char oxidation reaction.

to 0.583 s. The relative variation of the char burning time without the gas temperature fluctuation is 44.66% as the relative variation of the activation energy is 3.9%, and the relative variation of that is 130.43% as the relative variation of the activation energy is 9.09%. The corresponding instantaneous char oxidation reaction rates can be found in Fig. 3. The char oxidation reaction rates with the gas temperature fluctuation are greatly different from those without the gas temperature fluctuation. The instantaneous char oxidation reaction rate without the gas temperature fluctuation varies smoothly, while the gas temperature fluctuation leads to the fluctuation in the char oxidation reaction rate. The fluctuating variation of the char oxidation reaction rate exhibits more strongly as the fluctuation amplitude of the gas temperature increases. The increased values of the fluctuation peak are greater than the decreased values of the fluctuation trough. As a result, the average char oxidation reaction rate with the gas temperature fluctuation is greater than that without the gas temperature fluctuation. Also, the char oxidation reaction rate becomes greater as the activation energy of char oxidation reaction decreases, which directly leads to a faster NO release rate and a shorter char burning time.

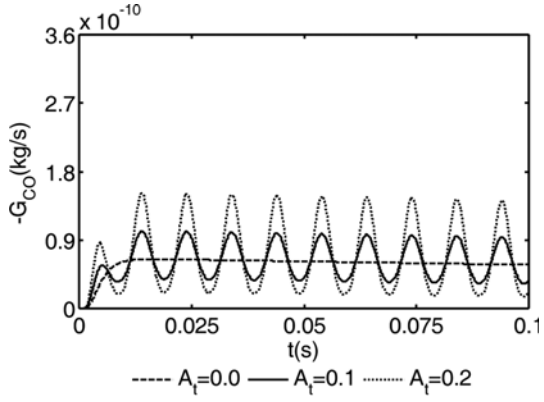

(a) B_{CO} = 400kg/(m^2·s·atm)

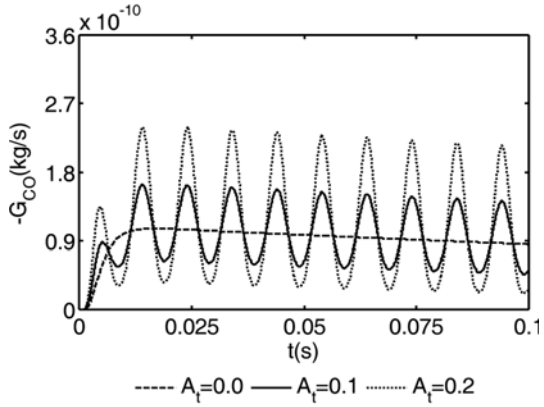

(b) B_{CO} = 600kg/(m^2·s·atm)

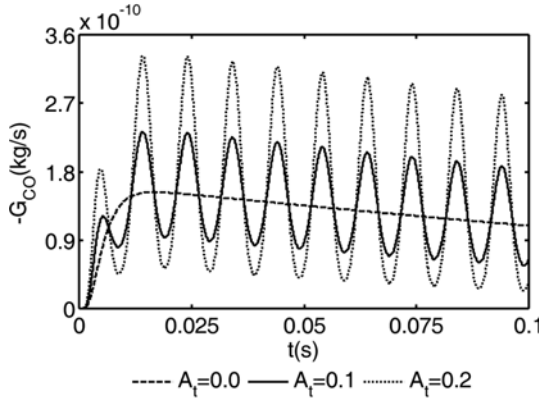

(c) B_{CO} = 800kg/(m^2·s·atm)

Fig. 5. Instantaneous char oxidation reaction rate under different pre-exponential factors of char oxidation reaction.

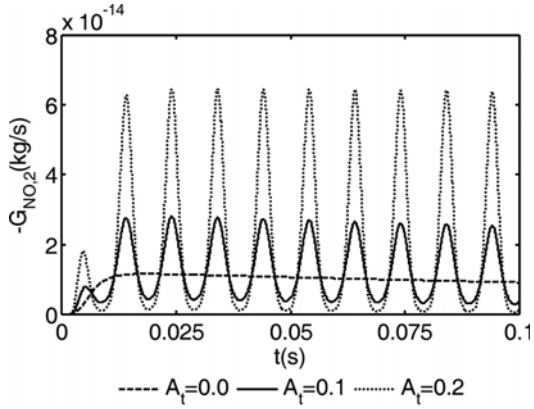

(a) $E_{NO,2}$ = 138kJ/mol

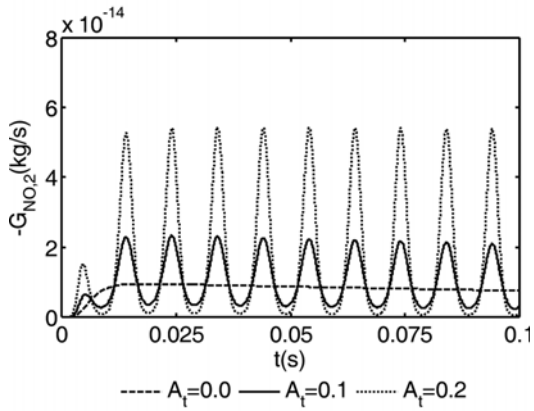

(b) $E_{NO,2}$ = 140kJ/mol

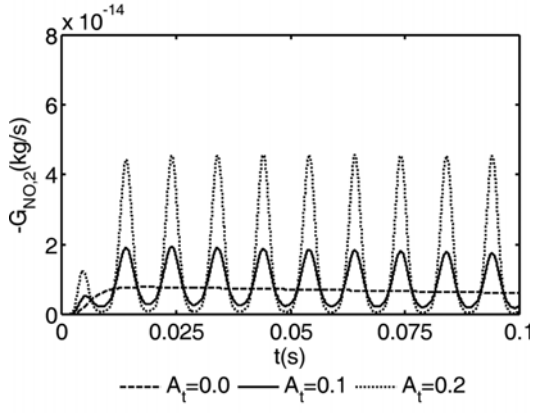

(c) $E_{NO,2}$ = 142kJ/mol

Fig. 6. Instantaneous NO reduction reaction rate under different activation energies of NO reduction reaction.

Fig. 4 presents the instantaneous released NO mass under the pre-exponential factor of char oxidation reaction of 400 kg/(m^2·s·atm), 600 kg/(m^2·s·atm), and 800 kg/(m^2·s·atm), respectively. The other kinetic parameters are given as E_{CO}=80 kJ/mol, $E_{NO,2}$=140 kJ/mol, and $B_{NO,2}$=40 kmol/(m^2·s·atm). The effect of the gas temperature fluctuation on the released NO mass under different pre-exponential factors of char oxidation reaction is the same as that under different activation energies of char oxidation reaction. With the increasing pre-exponential factor of char oxidation reaction, the released NO mass increases faster and the time for char burning is shorter. Compared with the char burning time under the pre-exponential factor of 400 kg/(m^2·s·atm), the relative variation of the conversion time without the gas temperature fluctuation is 37.44% as the relative variation of the pre-exponential factor is 50%, and the relative time variation is 56.41% as the relative variation of the pre-exponential factor is 100%. This is because the instantaneous char oxidation reaction rate increases with the increasing pre-exponential factor of char oxidation reaction, as can be seen from Fig. 5.

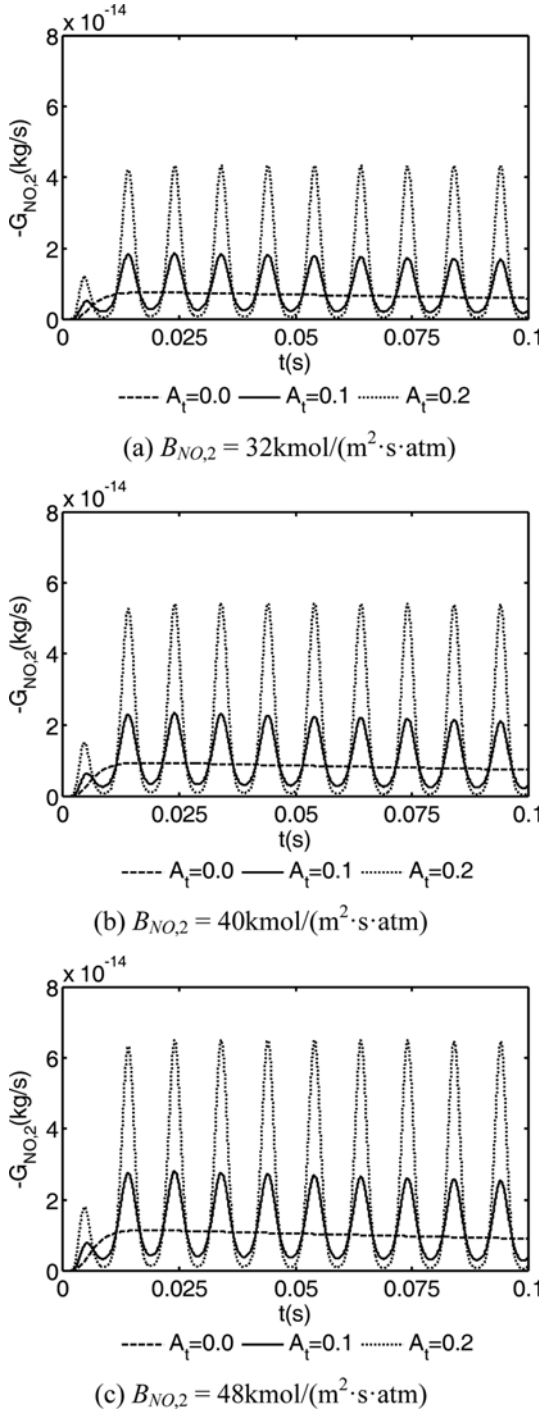

Fig. 7. Instantaneous NO reduction reaction rate under different pre-exponential factors of NO reduction reaction.

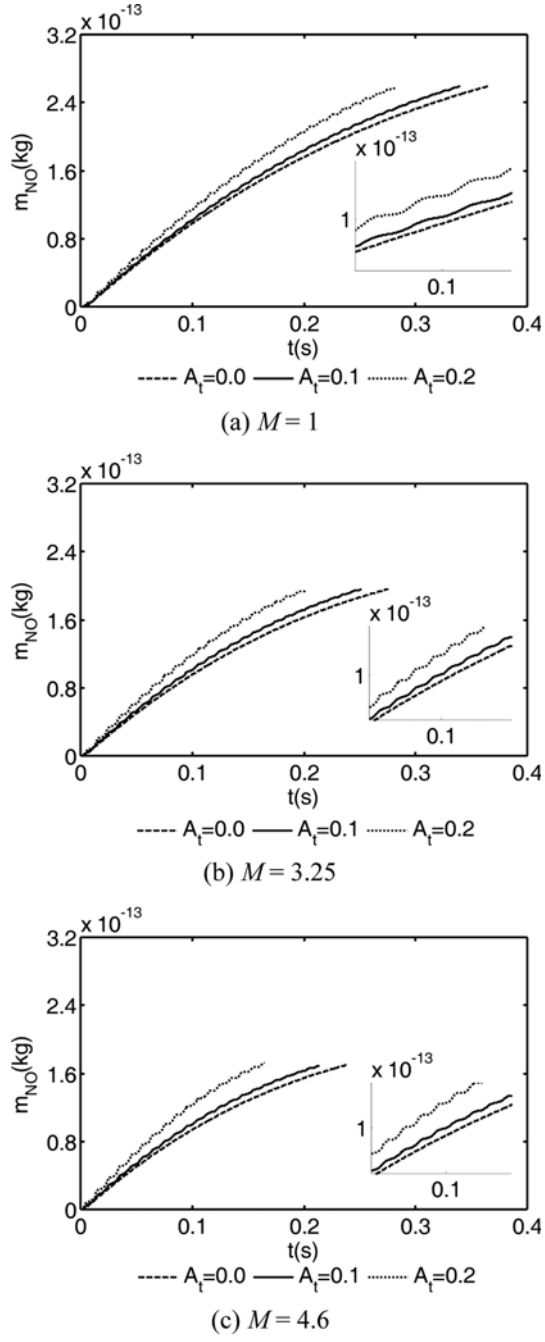

Fig. 8. Instantaneous released NO mass under different aspect ratios.

The effect of the kinetic parameters of NO reduction reaction on the char combustion processes can be found in Figs. 6-7. Fig. 6 shows the instantaneous NO reduction reaction rate under the activation energy of NO reduction reaction of 138 kJ/mol, 140 kJ/mol, and 142 kJ/mol, respectively. The other kinetic parameters are given as E_{CO}=80 kJ/mol, and B_{CO}=600 kg/(m^2·s·atm), and $B_{NO,2}$=40 kmol/(m^2·s·atm). Fig. 7 shows the instantaneous NO reduction reaction rate under the pre-exponential factor of NO reduction reaction of 32 kmol/(m^2·s·atm), 40 kmol/(m^2·s·atm), and 48 kmol/(m^2·s·atm), respectively. The other kinetic parameters are given as E_{CO}=80 kJ/mol, B_{CO}=600 kg/(m^2·s·atm), and $E_{NO,2}$=140 kJ/mol. The gas temperature fluctuation has a similar effect on the instantaneous NO reduction reaction rate. The increase of the activation energy of NO reduction reaction or the decrease of the pre-exponential factor of NO reduction reaction leads to an obvious decrease in the instantaneous NO reduction reaction rate. It is observed that the order of magnitude of the instantaneous NO reduction reaction rate in this computation is 10^{-14}, while the order of magnitude of the char oxidation reaction rate is 10^{-10}. As a result, the variations

of the kinetic parameters of NO reduction reaction have little effect on the instantaneous released NO mass variations and the time for char burning.

Fig. 8 presents the instantaneous released NO mass under the particle aspect ratio of 1, 3.25, and 4.6, respectively. The kinetic parameters are given as E_{CO}=80 kJ/mol, B_{CO}=600 kg/(m^2·s·atm), $E_{NO,2}$=140 kJ/mol, and $B_{NO,2}$=40 kmol/(m^2·s·atm). The increasing aspect ratio results in a faster released NO mass rate and a shorter char burning time. The time for char burning is 0.366 s, 0.276 s, 0.238 s, respectively. The relative variation of the conversion time without the gas temperature fluctuation is 24.59% as the relative variation of the aspect ratio is 225%, and the relative variation of that is 34.97% as the relative variation of the aspect ratio is 360%. This is because the primary influencing factor, the instantaneous char oxidation reaction rate, increases with the increasing aspect ratio, as indicated by Fig. 9. Clearly, the effect of the activation energy of char oxidation reaction on the char combustion processes is most significant. The pre-exponential factor of char oxidation reaction and the aspect ratio have distinct influences on the chemical conversion processes, while the kinetic parameters of NO reduction reaction have no obvious effect on the conversion time.

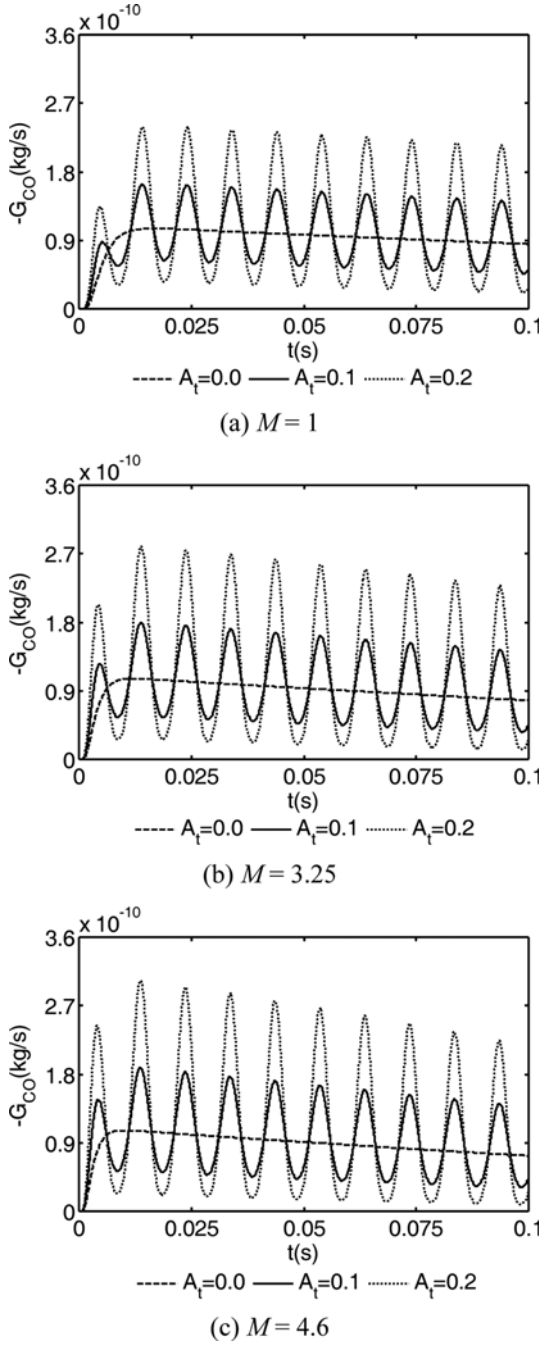

Fig. 9. Instantaneous char oxidation reaction rate under different aspect ratios.

CONCLUSION

We have investigated, numerically, the instantaneous heterogeneous reactions that involve the char oxidation reaction, the char nitrogen oxidation reaction, and the NO_x reduction reaction processes of prolate spheroidal particles suspended in a hot air flow with temperature fluctuation. The effects of the gas temperature fluctuation, the kinetic parameters (activation energy and pre-exponential factor) of char oxidation reaction and NO reduction reaction, and the particle aspect ratio on the NO release from ellipsoidal particles during char combustion were studied and the following conclusions reached:

(a) The gas temperature fluctuation has vital effects on the instantaneous NO release variation, the char oxidation reaction rate, and the NO reduction reaction rate during the char combustion processes. The gas temperature fluctuation leads to a faster conversion of char nitrogen to NO, a faster char oxidation reaction rate, and a faster NO reduction reaction rate. An increase in the fluctuation amplitude of the gas temperature will further promote the NO release and the char oxidation reaction processes.

(b) An increase in the activation energy of char oxidation reaction or a decrease in the pre-exponential factor of char oxidation reaction results in a shorter NO release rate and a shorter char oxidation reaction rate. Compared with the kinetic parameters of NO reduction reaction and the particle aspect ratio, the influence of the activation energy of char oxidation reaction on the char combustion processes is most prominent.

(c) The NO reduction reaction rate decreases with the increasing activation energy or the decreasing pre-exponential factor of NO reduction reaction. The activation energy and the pre-exponential factor of NO reduction reaction exhibit little effects on the NO release rate.

(d) An increase in the particle aspect ratio leads to an increase in the NO release rate and reaction rates under the same particle surface area.

ACKNOWLEDGEMENT

This study was supported by the National Natural Science Foundation of China under Grant No. 51076082.

NOMENCLATURE

a, b, c : semi-axes of ellipsoidal particle [m]

A_t : fluctuation amplitude of gas temperature
B_{CO} : pre-exponential factor for char oxidation reaction [kg/(m^2·s·atm)]
B_k : nondimensional variation rate of particle mass
$B_{NO,2}$: pre-exponential factor for NO reduction reaction [kg/(m^2·s·atm)]
C_p : gas specific heat [J/(kg·K)]
C_{pk} : particle specific heat [J/(kg·K)]
d_k : diameter of spherical particle with the same surface area [m]
D : diffusion coefficient of gas species [m^2/s]
E_{CO} : activation energy for char oxidation reaction [kJ/mol]
$E_{NO,2}$: activation energy for NO reduction reaction [kJ/mol]
f : fluctuation frequency of gas temperature [Hz]
g : total mass flux on the ellipsoid surface [kg/(m^2·s)]
g_{OX} : oxygen mass flux on the ellipsoid surface [kg/(m^2·s)]
G : total mass flow rate [kg/s]
G_{CO} : char oxidation reaction rate [kg/s]
G_{NO} : total nitricoxide mass flow rate [kg/s]
$G_{NO,1}$: char nitrogen oxidation reaction rate [kg/s]
$G_{NO,2}$: NO reduction reaction rate [kg/s]
G_{OX} : oxygen mass flow rate [kg/s]
H_ξ, H_η, H_ζ: scale factors
m_k : particle mass [kg]
M : particle aspect ratio
Nu_k : particle Nusselt number
t : time [s]
T : gas temperature [K]
T_{av} : time-averaged gas temperature [K]
T_ξ, R_η, S_ζ: scale factors
T_k : particle temperature [K]
T_w : wall temperature [K]
x, y, z : cartesian coordinates [m]
Y_{NO} : NO mass fraction
Y_{OX} : oxygen mass fraction

Greek Letter

β_{CO} : mass stoichiometric ratio for char oxidation reaction
$\beta_{NO,1}$: mass stoichiometric ratio for char nitrogen oxidation reaction
$\beta_{NO,2}$: mass stoichiometric ratio for NO reduction reaction
ε_k : particle emissivity
ξ, η, ζ: ellipsoidal coordinates [m]
Π : surface of concentric ellipsoid
λ : gas thermal conductivity [W/(m·K)]
ρ : gas density [kg/m^3]
ρ_{pk} : particle material density [kg/m^3]

Subscript

s : particle surface
∞ : surrounding environment

REFERENCES

1. E. Houshfar, L. Wang, N. Vähä-Savo, A. Brink and T. Løvås, *Clean Technol. Environ.*, **16**, 1339 (2014).
2. K. Zhao, A. D. Jensen and P. Glarborg, *Energy Fuel*, **28**, 4684 (2014).
3. M. Sami, K. Annamalai and M. Wooldridge, *Prog. Energy Combust.*, **27**, 171 (2001).
4. L. S. Johanssona, C. Tullina, B. Leckner and P. Sjövalla, *Biomass Bioenergy*, **25**, 435 (2003).
5. P. O. Hedman and D. L. Warren, *Combust. Flame*, **100**, 185 (1995).
6. H. Zhang and J. Zhang, *Fuel*, **89**, 1177 (2010).
7. Q. Shang, J. Zhang and L. Zhou, *Fuel*, **84**, 2071 (2005).
8. H. Zhang and J. Zhang, *Combust. Flame*, **153**, 334 (2008).
9. J. Pang and J. Zhang, *J. Anal. Appl. Pyrol.*, **108**, 196 (2014).
10. J. Zhang and L. Zhou, *Fuel*, **80**, 289 (2001).
11. B. Goshayeshi and J. C. Sutherland, *Combust. Flame*, **161**, 1900 (2014).
12. A. Bharadwaj, L. L. Baxter and A. L. Robinson, *Energy Fuel*, **18**, 1021 (2004).
13. R. I. Backreedy, L. M. Fletcher, J. M. Jones, L. Ma, M. Pourkashanian and A. Williams, *P. Combust. Inst.*, **30**, 2955 (2005).
14. Q. Guo, X. Chen and H. Liu, *Fuel*, **94**, 551 (2012).
15. S. R. Gubba, L. Ma, M. Pourkashanian and A. Williams, *Fuel Process. Technol.*, **92**, 2185 (2011).
16. M. Mandø, L. Rosendahl, C. Yin and H. Sørensen, *Fuel*, **89**, 3051 (2010).
17. H. Cui and J. R. Grace, *Chem. Eng. Sci.*, **62**, 45 (2007).
18. J. Li and J. Zhang, *Combust. Sci. Technol.*, submitted.
19. S. R. Turns, *An Introduction to Combustion: Concepts and applications*, McGraw-Hill, New York (1996).
20. D. T. Grow, *Combust. Flame*, **80**, 209 (1990).
21. M. Momeni, C. Yin, S. K. Kær, T. B. Hansen, P. A. Jensen and P. Glarborg, *Energy Fuel*, **27**, 507 (2012).
22. M. Momeni, C. Yin, S. K. Kær and S. Lovmand Hvid, *Energy Fuel*, **27**, 1061 (2013).
23. J. M. Levy, L. K. Chana, A. F. Sarofima and J. M. Beéra, *Symposium (International) on Combustion*, **18**, 111 (1981).
24. J. M. Jones, P. M. Patterson, M. Pourkashanian, A. Williams, A. Arenillas, F. Rubiera and J. J. Pis, *Fuel*, **78**, 1171 (1999).
25. W. Wang, S. D. Brown, C. J. Hindmarsh and K. M. Thomas, *Fuel*, **73**, 1381 (1994).
26. L. D. Smoot and P. J. Smith, *Coal combustion and gasification*, Plenum Press, New York (1985).
27. S. J. Madden Jr., *Celestial Mechanics*, **2**, 217 (1970).

APPENDIX A

The purpose of this appendix is to provide the species mass conservation in steady flow in terms of ellipsoidal coordinates.

The ellipsoidal coordinates (ξ, η, ζ) can be transformed from the Cartesian coordinates (x, y, z) using the expressions as [27]

$$x^2=\frac{(a^2+\xi)(a^2+\eta)(a^2+\zeta)}{(a^2-b^2)(a^2-c^2)} \tag{A1a}$$

$$y^2=\frac{(b^2+\xi)(b^2+\eta)(b^2+\zeta)}{(b^2-a^2)(b^2-c^2)} \tag{A1b}$$

$$z^2=\frac{(c^2+\xi)(c^2+\eta)(c^2+\zeta)}{(c^2-a^2)(c^2-b^2)} \tag{A1c}$$

The formula $x^2/(a^2+\xi)+y^2/(b^2+\xi)+z^2/(c^2+\xi)=1$ gives concentric ellipsoids when ξ=constant. It corresponds to the ellipsoid surface

for ξ=0. The metric distance is written as

$$(ds)^2 = H_\xi^2(d\xi)^2 + H_\eta^2(d\eta)^2 + H_\zeta^2(d\zeta)^2 \quad (A2)$$

The scale factors H_ξ, H_η, and H_ζ can be expressed as

$$H_\xi = \frac{1}{2}\frac{\sqrt{(\xi-\zeta)(\xi-\eta)}}{R(\xi)} \quad (A3a)$$

$$H_\eta = \frac{1}{2}\frac{\sqrt{(\xi-\eta)(\eta-\zeta)}}{S(\eta)} \quad (A3b)$$

$$H_\zeta = \frac{1}{2}\frac{\sqrt{(\eta-\zeta)(\xi-\zeta)}}{T(\zeta)} \quad (A3c)$$

where R_ξ, S_η, T_ζ are defined as

$$R_\xi = \sqrt{(a^2+\xi)(b^2+\xi)(c^2+\xi)} \quad (A4a)$$

$$S_\eta = \sqrt{-(a^2+\eta)(b^2+\eta)(c^2+\eta)} \quad (A4b)$$

$$T_\zeta = \sqrt{(a^2+\zeta)(b^2+\zeta)(c^2+\zeta)} \quad (A4c)$$

The general vector form for species mass conservation in steady flow is expressed as [19]

$$\nabla\cdot(\rho u Y_{spe}) = \rho D\nabla^2 Y_{spe} \quad (A5)$$

where u and Y_{spe} are velocity vector and species mass fraction, respectively. It is assumed that all the vectors involved are functions of the single coordinate ξ. The convection term and the diffusion term in ellipsoidal coordinates can be respectively written as [27]

$$\nabla\cdot(\rho u Y_{spe}) = \frac{1}{H_\eta H_\zeta H_\xi}\frac{\partial}{\partial\xi}(\rho u_\xi Y_{spe} H_\eta H_\zeta) \quad (A6a)$$

$$\rho D\nabla^2 Y_{spe} = \frac{4\rho D R_\xi}{(\xi-\eta)(\xi-\zeta)}\frac{\partial}{\partial\xi}\left(R_\xi\frac{\partial Y_{spe}}{\partial\xi}\right) \quad (A6b)$$

Substituting Eqs. (A3) (A4) (A6) into Eq. (A5) and rearranging yields

$$\frac{\partial}{\partial\xi}(gY_{spe}R_\xi H_\xi) = \rho D\frac{\partial}{\partial\xi}\left(R_\xi\frac{\partial Y_{spe}}{\partial\xi}\right) \quad (A7)$$

where $g=\rho u_\xi$ denotes the mass flux on the ellipsoid surface. Eq. (A7) is the species mass conservation in terms of the ellipsoidal coordinate system.